ELSEVIER

Journal of Nuclear Materials 294 (2001) 288–298

journal of nuclear materials

www.elsevier.nl/locate/jnucmat

# Temperature-dependence of defect creation and clustering by displacement cascades in α-zirconium

F. Gao [a], D.J. Bacon [a,*], L.M. Howe [b], C.B. So [b,1]

[a] *Department of Engineering, Materials Science and Engineering, The University of Liverpool, Brownlow Hill, Liverpool L69 3GH, USA*
[b] *AECL, Chalk River Laboratories, Chalk River, Ont., Canada KOJ 1JO*

Received 19 June 2000; accepted 16 January 2001

**Abstract**

Molecular dynamics (MD) modelling has been employed to investigate the effect of lattice temperature on the production of vacancies and interstitials in the primary damage process of displacement cascades with energy up to 20 keV in α-zirconium. The final number of Frenkel pairs decreases with increasing temperature due to the increase in lifetime of the thermal spike at high temperature. The production efficiency behaves in a similar fashion to that simulated at 100 K, but it is reduced further and saturates at about 20% over the energy range considered at 600 K. The number and size of clusters, both vacancy and interstitial, are increased by increasing PKA energy, and the fraction of interstitials in clusters also increases with increasing lattice temperature. The interstitial clusters can glide back and forth by one-dimensional migration along the crowdion direction at 100 K, but small clusters of less than four SIAs can change their glide direction on and off basal-planes at 600 K. It is also observed that single interstitials and some small clusters can migrate along both $\langle 1\,1\,\bar{2}\,0\rangle$ and $\langle \bar{2}\,2\,0\,3\rangle$ directions at 600 K. Clusters containing up to 25 interstitials and 24 vacancies were formed by 20 keV cascades at 600 K, and almost all of the clusters have the form of a dislocation loop with Burgers vector $1/3\langle 1\,1\,\bar{2}\,0\rangle$. It was found that the 25-interstitial cluster is glissile and dissociates on the basal and prism-planes that form its glide cylinder. Collapse of the 24-vacancy cluster to a perfect vacancy dislocation loop was found to occur in the primary damage process due to the longer lifetime of the thermal spike at higher temperature. The results are discussed in terms of experimental data and compared with those simulated at 100 K. © 2001 Published by Elsevier Science B.V.

## 1. Introduction

Molecular dynamics (MD) computer modelling can provide information on the number of defects created by displacement cascades in metals and the clustering of both interstitials and vacancies that occurs during the lifetime of cascades [1–4]. Such knowledge is crucial for the successful prediction and assessment of materials performance in power reactor systems. A wide range of metals has been simulated in recent years, but has been concerned mainly with metals and alloys of the cubic crystal structure. HCP metals have received less attention, although alpha-zirconium (α-Zr) is important because of its use in fuel cladding, calandria tubes and pressure tubes in several current reactor systems [5,6]. One study of α-titanium [7] and two of α-zirconium [8,9] have been reported, but displacement cascades were modelled only at 100 K, whereas the operating temperature in real reactors is much higher, e.g. typically 300°C in pressurised water reactors. It is therefore of interest to extend the MD simulations to higher temperature to see how defect production and clustering in the primary damage state are affected by the ambient temperature. In the present work, cascades of up to 20 keV in energy have been simulated in a model of α-Zr at 600 K and the results are compared with those from the earlier studies for 100 K [8,9].

* Corresponding author. Tel.: +44-151 794 5384; fax: +44-151 794 4675.
*E-mail address:* djbacon@liv.ac.uk (D.J. Bacon).
[1] Present address: C.S. Scientific Consulting Ltd., 23 Knotty Pine Trail, Thornhill, Ont., Canada L3T 3W5.

0022-3115/01/$ - see front matter © 2001 Published by Elsevier Science B.V.
PII: S0022-3115(01)00483-4

The computational method used is summarised in Section 2. In order to simulate constant temperature of the bulk metal, a hybrid/MD model developed by Gao et al. [10] was employed, where the temperature of the boundary atoms is scaled based on the continuum description of the thermal conduction. The temperature distribution in the core of cascades is analysed in Section 3, and defect production is described in Section 4. Data on the clustering of interstitials and vacancies as a function of temperature are presented in Section 5, and the geometry of some large defect clusters is analysed in Section 6. The results are discussed and compared with experimental data in Section 7, and finally conclusions are given.

## 2. Computational methods

The MD program was that used in previous work [7,8]. Constant pressure and periodic boundary conditions were employed. The many-body interatomic potential for α-Zr derived by Ackland et al. [11] was used for the simulations, but modified for displacement damage modelling [8]. The point defect properties calculated with this potential are in reasonable agreement with other simulations, and the threshold displacement energy, $E_d$, computed by Wooding et al. [8] is close to the experimental values. The same potential has been used to simulate displacement cascades for primary-knock-on atom (PKA) energy, $E_p$, up to 20 keV at 100 K [9].

In order to treat the heat dissipation from a cascade into the surrounding material, the MD code was adapted using a model developed by Gao et al. [10] in which the MD crystal is embedded in a large continuum block. The continuum and MD iterations run in parallel, but at each time-step the velocity of atoms in the boundary region of the MD block is scaled so that the temperature distribution in this region matches the solution for that of the continuum supercells it coincides with. The continuum is divided into cubic cells of linear dimension $a$, and the temperature in each one at time $(t + \Delta t)$ is obtained from that at $t$ by solving the equation of heat conduction in an anisotropic medium in a discretised form [10]. The material properties enter through the parameter $\Delta t' = (\rho a^2/\kappa)$, where $\rho$ is the density and $\kappa$ the thermal conductivity. For the HCP structure there are two $\kappa$ constants, corresponding to conduction parallel and perpendicular to the [0 0 0 1]-axis.

We have simulated uniaxial heat flow in an elongated MD block to determine the thermal conductivities to be used in the continuum approximation of the real atomic system. For conductivity along the [0 0 0 1]-axis the block size was $6a_0 \times 4\sqrt{3}a_0 \times 158c_0$ (= 15168 atoms), where $a_0$ and $c_0$ are the HCP lattice parameters, and for heat flow parallel to the basal-plane it was $252a_0 \times 4\sqrt{3}a_0 \times 4c_0$ (= 12096 atoms). Periodic boundary conditions were imposed in all three directions. After the crystal was equilibrated at 100 K for 5 ps, an approximate Gaussian profile of temperature was introduced into the central region of the crystal via the atomic velocities, and then the block was equilibrated for a further 3 ps to establish the phonon modes. At this time, the block was notionally divided into supercells of size $6a_0 \times 6a_0 \times 6a_0$, each containing 360 atoms, and the temperature in each supercell was calculated to give the initial distribution of temperature for the continuum model. The continuum and MD iterations were then run in parallel for a period of 10–20 ps, and the value of $\Delta t'$ was determined from the condition that the temperature distribution calculated by the continuum model was approximately the same as that simulated by MD. Good agreement was found for $\Delta t' = 2.835$ and 2.238 ps for heat flow perpendicular and parallel to the [0 0 0 1]- (or $c$-) axis, respectively. The smaller value of $\Delta t'$ for the $c$-direction implies a higher value of $\kappa$ for the ionic system. This reflects the fact that $C_{33}$ is bigger than $C_{11}$. These values for $\Delta t'$ compare with an average value of 0.315 ps using the experimental $\kappa$ and $\rho$ values for metallic zirconium. This order-of-magnitude difference is expected because the electronic contribution to $\kappa$ is neglected in the MD model. However, unless the coupling between electrons and phonons is large, the electronic contribution to coupling should be small over the lifetime of the thermal spike of a cascade.

To simulate a cascade, the MD model was first equilibrated for at least 10 ps at the required irradiation temperature, $T_{irr}$, so that when the PKA event was initiated, the equilibrium phonon modes were already established. A cascade was started by imparting a kinetic energy $E_p$ to one atom, i.e. the PKA, following which the crystal was allowed to evolve for at least 1000–2000 timesteps (~10–20 ps). The crystallographic directions selected for the PKA were those used in the earlier studies of titanium and zirconium [7–9]. The crystal size was increased with increasing PKA energy so that 532,360 atoms were used for 20 keV cascades $(72a_0 \times 41\sqrt{3}a_0 \times 45c_0)$. Four to six simulations were run at each $E_p$ in order to generate sufficient statistics to indicate trends.

## 3. Temperature in the core of cascades

The analysis of temperature in the core of cascades, particularly in the zone within which the effective temperature exceeds the melting temperature, is useful for understanding the dynamic behaviour of cascades created at different temperature, and so we have analysed

the temperature profile in the core of two cascades in detail. The plots of Figs. 1(a) and (b) show the radial temperature profiles at different times during the thermal spike phase for a 20 keV cascade at each of the temperatures $T_{irr} = 100$ and 600 K, where data for 100 K has been obtained from the results of simulations in [9]. The temperature plotted is the mean value in spherical shells of thickness either 0.232 or 0.267 nm for 100 and 600 K, respectively, which are centred on the 'centre of gravity' of the displaced atoms at the time $t_{peak}$, defined as the time near the end of the collision phase at which the number of displaced atoms reaches a maximum. ( A 'displaced' atom at any instant is defined to be one which does not lie within a distance of $0.32a_0$ of a lattice site.) In the early stage of the thermal spike, the core region in both cascades attains a high effective temperature well above the melting temperature ($T_m = 2120$ K for the present model) of α-Zr, but during the next few picoseconds the core temperature decreases rapidly with time and then gradually returns to the ambient temperature. The maximum radius, $R_{melt}$, of the spherical zone within the effective temperature exceeds $T_m$ is plotted as a function of time in Fig. 2. It can be seen that this region is bigger by a factor of about 2 in size and 8 in volume for 600 K than for 100 K, and the time for it to shrink to a given size is much longer. This demonstrates that the thermal spike is likely to be more pronounced at 600 K than at 100 K for the same PKA energy. The extent of the difference is similar to that found in α-Fe [10] and $Ni_3Al$ [12] using similar boundary conditions.

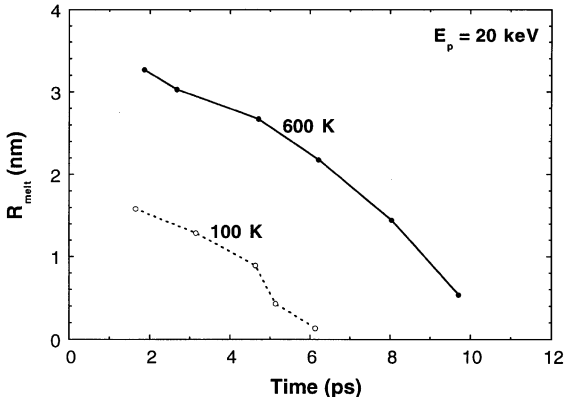


Fig. 2. Data for $R_{melt}$ defined in the text as a function of time for $T_{irr} = 100$ and 600 K.

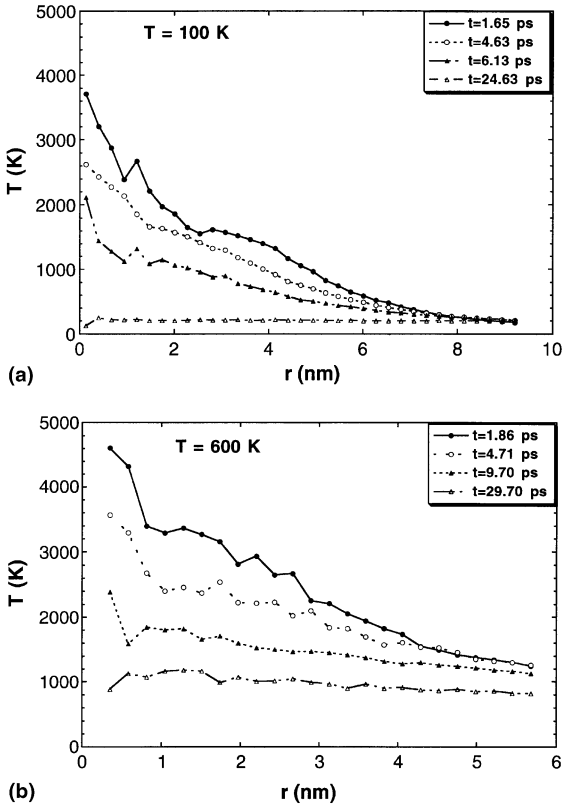


Fig. 1. The variation with time of the mean temperature in spherical shells of thickness; (a) 0.232 nm for 100 K, and (b) 0.267 nm for 600 K as a function of radial distribution from the cascade centre.

## 4. Defect production

In simple terms, the defect distribution in the final damage state of a cascade consists of the greater part of the self-interstitial atoms (SIAs) around the outside of the highly disordered core created in the thermal spike and the vacancies within this region. The final defect structure for typical cascades of 10–20 keV in a matrix at 600 K is plotted in Figs. 3(a) and (b), respectively. A feature that is apparent from the defect arrangements in Fig. 3 is that some large clusters of vacancies and of interstitials can be formed for both 10 and 20 keV. Simulations for iron [10] showed that the proportion of defects in clusters in that metal increases with increasing $T_{irr}$, and a cursory assessment of the cascade damage observed in the present work suggests that the same effect occurs in zirconium.

Data for the final number of Frenkel pairs, $N_F$, at the end of the cascade process in zirconium at 600 K are plotted logarithmically as a function of energy in Fig. 4. The line joining the points denotes the means, and the bars indicate the standard error. Data obtained at 100 K [9] are also included. The heat dissipation conditions described in Section 2 were not applied in [9]: the MD model was adiabatic. However, the simulations of tem-

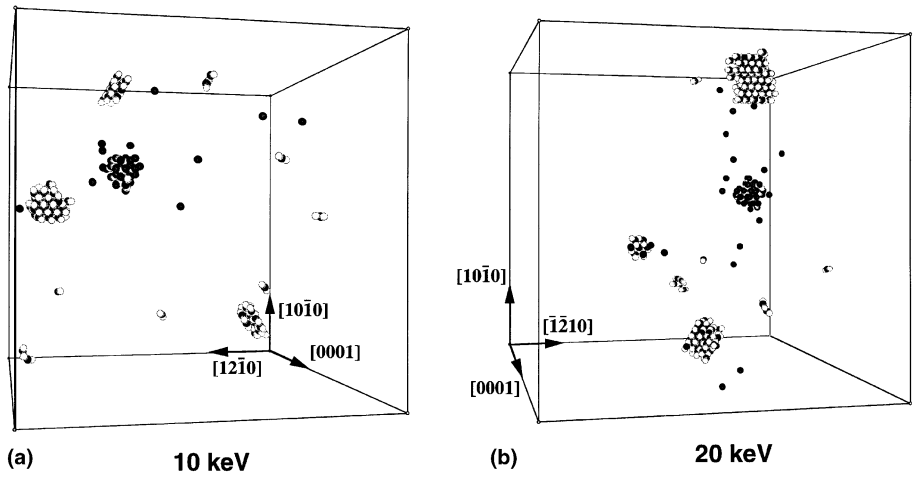


Fig. 3. Computer plots showing the final state of damage of; (a) a 10 keV cascade, and (b) a 20 keV cascade at 600 K, where white spheres represent interstitials and dark spheres indicate vacancies.

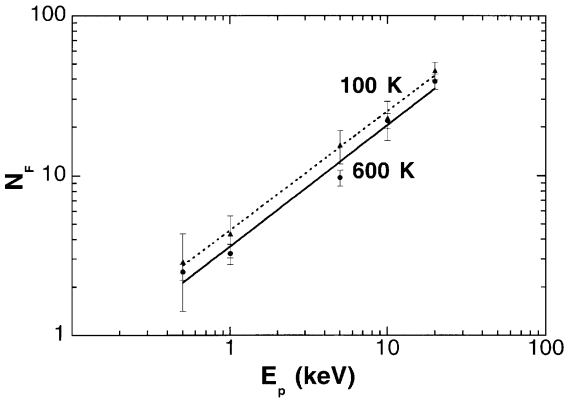


Fig. 4. Variation of $N_F$ with $E_p$ at 100 and 600 K using logarithmic scales, where the data points are the mean values over all the cascades at each energy and the bars denote the standard error.

perature effects in iron [10] demonstrated quantitatively that the results investigated by MD without damping the boundaries are acceptable so that the rise in temperature associated with $E_p$ is small. It is reasonable, therefore, to compare the present results with those in [9]. Although $N_F$ increases with increasing energy, as expected, it decreases with increasing temperature at all energies considered here. This is due to the increase in the lifetime of the thermal spike at high temperature (Fig. 2), which results in more SIA–vacancy recombination before cooling.

As reviewed elsewhere [3,4], the final number of defects produced in cascades is an important parameter for theories of radiation-damage evolution, and has long been based on the NRT formula [13]

$$N_{NRT} = 0.8E_{dam}/2\bar{E}_d, \quad (1)$$

where $E_{dam}$ is the energy of the primary recoil atom dissipated elastically in collisions ($= E_p$ in our case) and $\bar{E}_d$ is the mean threshold displacement energy. However, MD simulations have shown that the production efficiency of Frenkel pairs is considerably smaller than that predicted by the NRT standard. To show this, we compare the values of $N_F$ at 100 and 600 K with the NRT prediction by plotting $N_F/N_{NRT}$ against $E_p$ in Fig. 5. In the calculation of $N_{NRT}$, we took $\bar{E}_d$ to be 40 eV, which is close to the spatial means in the MD models [8] and the value specified in the NRT standard (Standard E521-89, Annual Book of ASTM Standards, ASTM, Philadephia, PA, USA). It can be seen that $N_F/N_{NRT}$ behaves in a similar

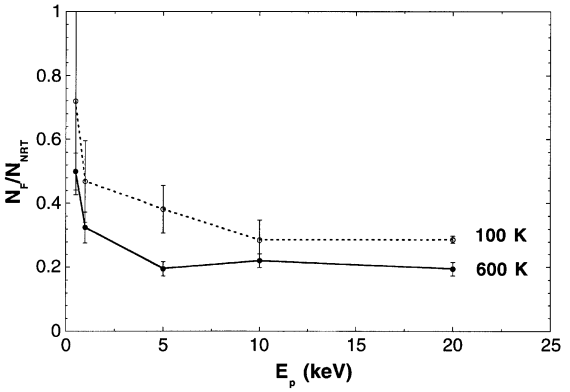


Fig. 5. Variation of the ratio $N_F/N_{NRT}$ with the primary recoil energy $E_p$ for 100 and 600 K, where the data points are the mean values over all the cascades and the bars denote the standard deviation. $\bar{E}_d$ was taken as 40 eV in calculating $N_{NRT}$.

fashion to that reported for metals of other crystal structures at 100 K. When the initial lattice temperature is increased to 600 K, the production efficiency (relative to the NRT estimate) is reduced further and saturates at about 20% over the energy range considered.

For all the metals simulated to date, including α-Zr, it has been shown that $N_F$ has a power-law dependence on $E_p$ [2–4,7,9]:

$$N_F = A(E_p)^m, \tag{2}$$

where $A$ and $m$ lie in the ranges 4–8 (with $E_p$ in keV) and 0.7–0.8, respectively. The value of $m$ less than one reflects the decreasing efficiency of defect production as $E_p$ increases. The new data for Zr reported here fit this relationship well, as shown by the logarithmic plots in Fig. 4. The best-fit values of $A$ are 4.57 and 3.61 keV$^{-m}$ at 100 and 600 K, respectively, and the corresponding values of $m$ are 0.741 and 0.757.

## 5. Defect clustering

The tendency of defects to cluster within their parent cascade is important because it affects the way they behave and contribute to microstructure evolution [14]. Data for the final cluster distribution of interstitial defects, averaged over all the cascades at 600 K, are plotted in the form of histograms as a function of the energy in Fig. 6, together with those at 100 K [9]. (We define an interstitial cluster such that within it, every SIA has at least one nearest-neighbour SIA.) It is clear that the number and size of SIA clusters increase with the energy, so that at 20 keV an appreciable fraction of the SIAs are produced in cluster form, i.e. 125 out of 154 of the SIAs found on the average in the cascades were in clusters of two or more interstitials. The largest cluster at 600 K was 25 for 20 keV cascades and 11 for 10 keV, which is very similar to the size at 100 K.

The reduction in the number of single interstitials at high temperature is clear from this plot, i.e. there is an increase in the interstitial clustering fraction, $f_i^{cl}$, defined as the ratio of surviving interstitials that are found in clusters of size two or larger to the total number of interstitials produced in a cascade. This parameter was calculated as a function of $T_{irr}$ and $E_p$ for α-Fe using the conventional MD model by Phythian et al. [15] and the MD/continuum hybrid model by Gao and Bacon [10]. For the present work, we have gone further and determined $f_i^{cl}$ in zirconium for clusters of minimum size 2, 3 or 4 SIAs. The results are shown as a function of PKA energy for 600 K in Fig. 7,

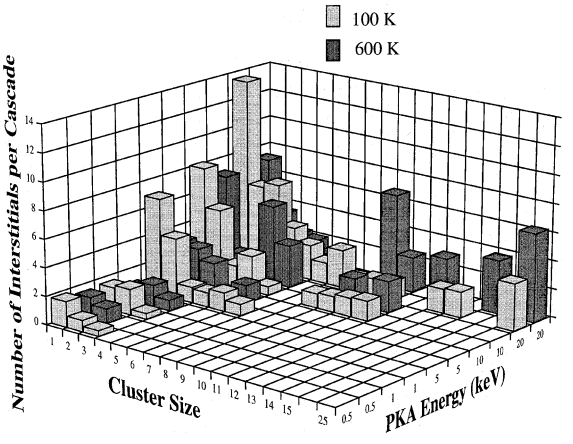


Fig. 6. Data for the number of single and clustered SIAs per cascade as a function of cascade energy $E_p$ for 100 and 600 K. The data were obtained by averaging over all cascades at each energy.

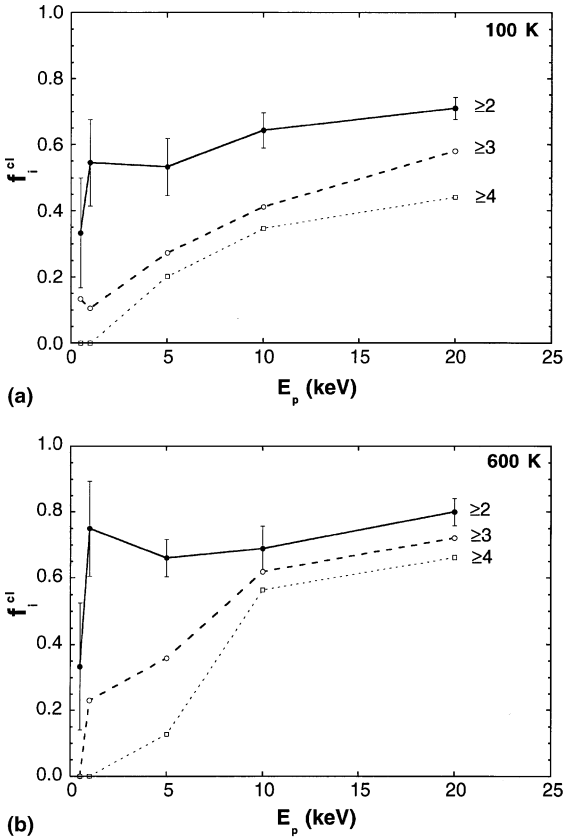


Fig. 7. The fraction, $f_i^{cl}$, of SIAs that survive in clusters of two or more, three or more, and four or more for (a) 100 K and (b) 600 K.

together with data extracted from the earlier simulations at 100 K. The points represent the mean values and the bars indicate the standard error. It is clear that the interstitial clustering fraction increases steadily with increasing $E_p$ for both temperatures, but $f_i^{cl}$ for 600 K is greater than that for 100 K over the whole energy range considered. This trend is consistent with the results of simulations for α-Fe [10,15] and is believed to be due to the larger lifetime of the thermal spike at the higher temperature.

From Fig. 3 it is clear that small clusters of interstitials have the form of parallel crowdions with their axis along a $\langle 11\bar{2}0\rangle$ direction, and large clusters are akin to perfect dislocation loops with a Burgers vector $\mathbf{b} = 1/3\langle 11\bar{2}0\rangle$ for both temperatures. In visualisations of their behaviour in MD simulations, they can be seen to glide back and forth by one-dimensional migration along the crowdion direction. However, single interstitials and small clusters of two or three interstitials occasionally migrate along $\langle\bar{2}203\rangle$ directions at 600 K, the relative difficulty of these non-basal steps perhaps reflecting the fact that the formation energy of the basal $\langle 11\bar{2}0\rangle$ crowdion and the $\langle\bar{2}203\rangle$ pseudo-crowdion is 3.77 and 4.00 eV, respectively. Thus, small clusters can change their glide direction on and off the basal-planes and migrate three dimensionally at high temperature. This is consistent with the MD study using the same interatomic potential by Whiting and Bacon [16], who investigated the migration of single interstitials and small interstitial clusters in α-zirconium at different temperatures (100–900 K) over much longer times than those used here. The fraction of SIAs in clusters of minimum size three and four is also plotted as a function of PKA energy in Figs. 7(a) for 100 K and (b) for 600 K. These plots reveal the importance of the energy spectrum in determining the fraction of the interstitials in clusters of a given minimum size, and thus in determining the fraction of the clusters that are able to migrate three dimensionally. The effect of the increase in $T_{irr}$ from 100 to 600 K is to suppress the difference between the different cluster fractions for $E_p \geqslant 10$ keV.

Vacancy clusters can also form in the centre of cascades. From a similar analysis to that for interstitials, the final number and cluster distribution of vacancy defects are plotted in the form of histograms as a function of the primary recoil energy in Fig. 8. Although the number and size of vacancy clusters increases with energy, the tendency for vacancy clustering is approximately the same for 100 and 600 K. The largest cluster was 24 for 20 keV cascades and 15 for 10 keV at 600 K. In a similar fashion to $f_i^{cl}$, the vacancy clustering fraction, $f_v^{cl}$, is defined to be the fraction of surviving vacancies found in clusters of size two or larger, and is shown as a function of PKA energy for 600 K in Fig. 9, together with data extracted from the simulations at 100 K. The points represent the mean values and the bars indicate the standard error. The vacancy clustering fraction increases steadily with increasing $E_p$ for both temperatures and appears to saturate at about 0.5 for $E_p = 10$ keV. Thus, although larger vacancy clusters are found in the higher energy cascades, the fraction of vacancies in clusters is approximately constant. Also, the vacancy clustering fraction appears to be the same at 100 and 600 K. This is believed to be due to the fact that the migration of vacancies and vacancy clusters does not occur after the molten core has solidified, and so the irradiation temperature does not have a significant influence on the vacancy clustering in the primary cascade damage.

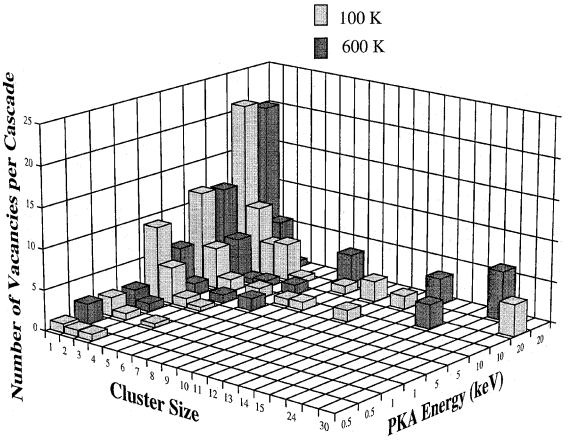


Fig. 8. Data for the number of single and clustered vacancies per cascade as a function of cascade energy $E_p$ for 100 and 600 K. The data were obtained by averaging over all cascades at each energy.

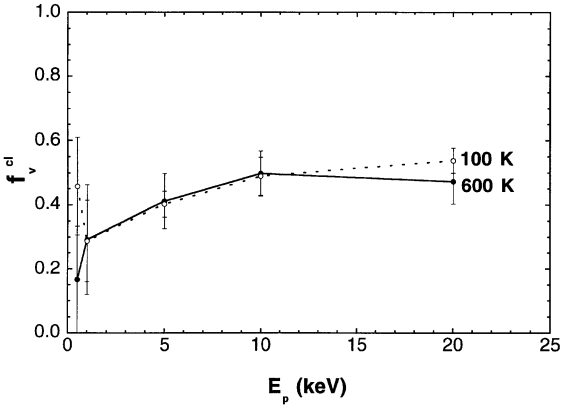


Fig. 9. The fraction, $f_v^{cl}$, of vacancies in clusters of size two or more per cascade as a function of cascade energy $E_p$ for 100 and 600 K. The data were obtained by averaging over all cascades at each energy.

## 6. Geometry of the large defect clusters

### 6.1. Interstitial clusters

In the earlier simulations of low energy ($E_p \leqslant 5$ keV) cascades in both zirconium and titanium [7,8] at 100 K, it was found that small clusters of interstitials in their stable state consist of parallel crowdions in the basal-plane with axis along one of the close-packed directions $\langle 1\,1\,\bar{2}\,0\rangle$. They approximate to glissile dislocation loops with Burgers vector $\mathbf{b} = 1/3\langle 1\,1\,\bar{2}\,0\rangle$. Wooding et al. [9] recently investigated high energy cascades (up to 20 keV) at 100 K in Zr, and found that although most SIA clusters had this form, the largest cluster, consisting of 25 interstitials, did not have a structure characteristic of dislocations expected in the HCP lattice, and did not achieve this stable state during annealing for 110 ps. It is therefore of interest to consider the nature of the larger clusters created in the present work.

In striking coincidence with the results for 100 K, the largest cluster found in present work again consisted of 25 interstitials. It is shown near the top in Fig. 3(b). It occupies sites in four adjacent basal-planes and, whereas the cluster at 100 K was a metastable arrangement that did not achieve the stable dislocation state, the 25-interstitial defect at 600 K had established an identifiable dislocation structure at the end of the thermal spike. To demonstrate this, the MD block was quenched to 0 K, and the atomic arrangement in either basal-plane or prism-plane projections through the centre of the cluster is plotted in Figs. 10(a) and (b). These plots show that the dislocation core surrounding the cluster is extended along the $[\bar{1}\,2\,\bar{1}\,0]$ glide cylinder, as indicated by the dislocation symbols which show where the difference in displacement between atoms inside and outside the cylinder is either b/4 or 3b/4. They indicate a tendency for the core to dissociate on the basal-plane into two Shockley partials bounding a ribbon of $I_2$ fault (Fig. 10(a)) according to the reaction

$$\frac{1}{3}[\bar{1}\,2\,\bar{1}\,0] = \frac{1}{3}[\bar{1}\,1\,0\,0] + \frac{1}{3}[0\,1\,\bar{1}\,0], \tag{3}$$

and to extend on the prism-plane (Fig. 10(b)) by the reaction

$$\frac{1}{3}[\bar{1}\,2\,\bar{1}\,0] = \frac{1}{6}[\bar{1}\,2\,\bar{1}\,0] + \frac{1}{6}[\bar{1}\,2\,\bar{1}\,0]. \tag{4}$$

However, in neither case is a true, stable stacking fault formed. The difference in form for the clusters of the same size at 100 and 600 K may reflect the importance of temperature in allowing defects to attain their equilibrium state. In the present study, it is of interest to note that the 25-interstitial cluster is mobile and can glide back and forth along the $[\bar{1}\,2\,\bar{1}\,0]$ direction during the thermal spike phase.

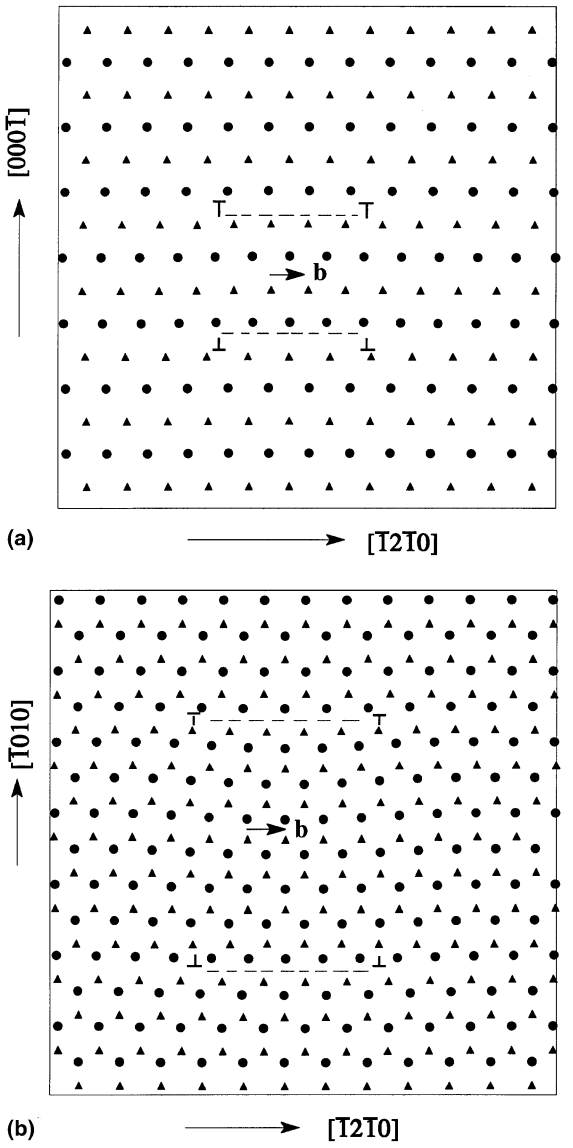


Fig. 10. (a) $[\bar{1}\,0\,1\,0]$ projections of the atomic positions in two basal-planes, and (b) $[0\,0\,0\,1]$ projections of the atomic positions in two prism-planes through the 25-interstitial cluster shown in Fig. 3(b). The broken lines indicate the dissociation of the cluster on the basal and prism-planes.

### 6.2. Vacancy clusters

In simulations of displacement cascades at 100 K [9], none of the vacancy clusters formed dislocation loops by cascade collapse. Since the lattice around the largest cluster was considered to have the greatest chance of collapsing to a dislocation configuration, the atomic arrangement of a 30-vacancy cluster at the end of the thermal spike was analysed and found to have a three-dimensional, hybrid form consisting of a conventional

prism-plane dislocation loop in its upper portion and a (0 0 0 1) stacking-fault at the bottom. Over the time of an additional simulated anneal of 110 ps, it changed to become a more-clearly defined faulted loop in the $(1\bar{1}00)$ prism-plane with a $1/2[\bar{1}100]$ Burgers vector. This is consistent with the crystallography of the majority of small vacancy loops observed by TEM in thin foils of ion-irradiated HCP metals, including titanium and zirconium [17]. Thus, it is of interest to consider the nature of the largest cluster of 24 vacancies found in a 20 keV cascade and seen in the centre of Fig. 3(b).

The atomic positions in [0 0 0 1] projection in two adjacent basal-planes are plotted in Figs. 11(a) and (b), where some near-neighbour bonds have been sketched to attempt to provide an interpretation of the structure. It can be seen that the six and five vacancies in Figs. 11(a) and (b) have created a configuration consistent with removal of part of a $(\bar{1}010)$-plane and collapse of the surrounding atoms into the hole. The projection shows the standard vacancy dislocation loop form with a partial Burgers vector $\mathbf{b} = 1/2[\bar{1}010]$ as indicated. The configuration in (b) exhibits some shear displacements parallel to the loop-plane, corresponding to unfaulting to $\mathbf{b} = 1/3[\bar{2}110]$. The collapse of the vacancy cluster to a vacancy loop occurred during the thermal spike phase, unlike that of the 30-vacancy cluster at 100 K. Again, the reason is believed to be that the lifetime of the thermal spike at 600 K is much longer than at 100 K, thus increasing the chance of collapse.

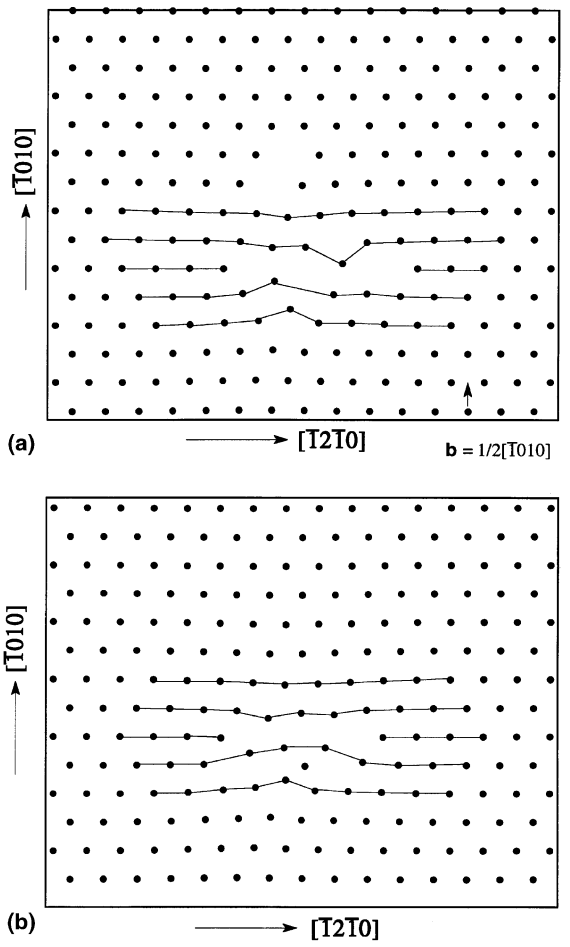


Fig. 11. Projections of the atomic positions in two planes through the 24-vacancy cluster shown in Fig. 3(b). The lines sketched on the figures reveal the character of the vacancy dislocation loop.

## 7. Discussion

The purpose of the present simulations was to investigate the effect of lattice temperature on the defect production and clustering in the primary damage process associated with displacement cascades in α-Zr. The emphasis was on the effects of the longer lifetime of the thermal spike at high temperature. It has been shown quantitatively in Figs. 1 and 2 how the size and lifetime of the 'molten' zone is affected by the lattice temperature. As a result, the final number of Frenkel pairs decreases as temperature increases, to a similar extent to α-Fe [10], because the increasing lifetime of the thermal spike allows more interstitials to recombine with vacancies. The data of Fig. 6 suggest that single interstitials dominate the recombination. Furthermore, cascades at high temperature are more compact because of a shortening of focused collision sequences due to the increasing amplitude of atomic vibrations, and this reduces the separation of interstitials and vacancies. The size of interstitial clusters and the clustering fraction increase with increasing temperature as shown in Figs. 6 and 7. It was found in [9] that the movement of small interstitial clusters at 100 K is largely restricted to $\langle 11\bar{2}0\rangle$ paths in the basal-plane, and most of the large interstitial clusters are glissile loops with perfect $1/3\langle 11\bar{2}0\rangle$ type Burgers vector. At 600 K, the large interstitial clusters exhibit similar behaviour to those at 100 K, but the small clusters of less than four SIAs show different migration paths. As described in Section 5, small clusters can migrate along both $\langle 11\bar{2}0\rangle$ and $\langle\bar{2}203\rangle$ directions at 600 K, and therefore change the dimensionality of their motion. This may be important in subsequent evolution of the microstructure because of the different kinetics of their interaction with other components of the microstructure [18]. Figs. 7(a) and (b) also illustrate the influence of the PKA energy on the fraction of SIA clusters of a given minimum size, and hence on the fraction that exhibits three- or one-dimensional motion. For $E_p$ less than 5–10 keV, most of the primary clusters are of size 2 or 3 and can migrate three dimensionally, whereas at higher energy most are

of size 4 or larger and are restricted to one-dimensional motion. The increase in $T_{irr}$ accentuates this effect because single interstitials and small clusters move to form one-dimensional clusters in the longer thermal spike at high temperature. The number and size of vacancy clusters increases with the energy, but is similar for 100 and 600 K. Since the present study was concerned with the primary damage state, the crystal was allowed to evolve for only a few tens of ps, within which the migration of vacancies does not occur at the ambient temperature. Vacancy clusters are mainly formed early in the thermal spike phase and the ambient temperature has no significant influence on the clustering, for the probability of a vacancy jumping within a period of, say, 10 ps is effectively zero at 600K, whereas the jump frequency of a self-interstitial is of the order of 0.5 $ps^{-1}$ at the same temperature [16].

Despite the variability in cascade form and defect production, the power-law dependence of the mean value of $N_F$ on $E_p$, first found empirically in [2] from MD data for cascades at low energy, holds for α-zirconium for $E_p$ up to 20 keV for irradiation temperatures of 100 and 600 K. As a result, $N_F$ in this metal is $\leqslant 25\%$ of the NRT estimate for cascade up to 20 keV at both temperatures. In the present state of knowledge, it is not possible to state what proportion of the $N_F$ interstitials actually leave the cascade region and become freely migrating defects. This will depend upon the extent to which intracascade SIA–vacancy recombination and entrapment of migrating interstitial clusters actually occur, and the simulation of this is beyond the MD timescale. However, the fact that $N_F$ is 25% of $N_{NRT}$ and the clustering fraction of SIAs is large (Fig. 7) suggests that the number of freely migrating defects is less than 10% of the NRT value in zirconium.

Irrespective of the temperature, some interstitial clusters do not have a simple structure and form metastable configurations as decribed by Wooding et al. [7,8]. It is of interest to note that Gao et al. [19] found that sessile, metastable clusters of interstitials are created in MD simulations of cascades in α-iron at both 100 and 600 K. Their thermal stability was investigated, and most transform to the glissile, stable state within a few hundred ps at about 500 K, with an activation energy of between 0.35 and 0.5 eV. This result and the present observations suggest that metastable arrangements of interstitial clusters can exist for a considerable time after the cascade event in irradiated metals.

The largest interstitial cluster (25 interstitials) was found to extend on the basal and prism-planes, and can migrate along the $[\bar{1}2\bar{1}0]$ glide cylinder. Osetsky et al. [20] carried out extensive studies of the mobility of interstitial clusters in fcc Cu, and found that the perfect loops with the Burgers vetctor $\mathbf{b} = 1/2\langle 1\,1\,0\rangle$ containing more than 64 interstitials dissociate on their glide prism. This restricts their thermally-activated motion. Thus, it would be interesting to investigate the behaviour and mobility of the large interstitial clusters in hcp metals and to compare them with those found in Cu.

Experiments on neutron-irradiated zirconium [21] have shown that damage is a complex function of irradiation temperature and purity. For irradiation below 673 K, it consists of loops with Burgers vector of $\mathbf{b} = 1/3\langle 1\,1\,\bar{2}\,0\rangle$, and for irradiation temperature between 673 and 773 K vacancy and interstitial loops with $\mathbf{b} = 1/3\langle 1\,1\,\bar{2}\,0\rangle$ are the predominant defects, but $1/6\langle 2\,0\,\bar{2}\,3\rangle$ vacancy loops and voids have been observed. The interpretation of the microstructure developed during irradiation in zirconium found that vacancy and interstitial dislocation loops with Burgers vector $\mathbf{b} = 1/3\langle 1\,1\,\bar{2}\,0\rangle$ coexist during neutron and electron irradiation [22,23]. The stability of large vacancy loops is dependent on the temperature. They are unstable at temperature above ~723 K because of vacancy thermal emission and may not be produced at temperature below ~353 K. Between 573 and 723 K there are approximately equal numbers of both types in the centre of large grains of annealed materials following neutron irradiation. Vacancy loops with $\mathbf{b} = 1/6\langle 2\,0\,\bar{2}\,3\rangle$ have been also observed in zirconium and zirconium alloys following neutron irradiation at 560 and 773 K. Their stability is dependent to a large extent on the presence of solute elements, which may have effects such as a lowering of the stacking-fault energy or a change in the vibration modes (and thus the cooling of the thermal spike) or the formation of solute-defect complexes.

Although the PKA energy range for the present simulations is below that used to create visible defects in the experiments, the MD results presented here are consistent qualitatively with general observations described above. The interstitial clusters were found to be predominantly prism-plane dislocation loops with Burgers vector $\mathbf{b} = 1/3\langle 1\,1\,\bar{2}\,0\rangle$ at both 100 and 600 K. This is entirely consistent with the experimental findings. Large vacancy clusters were observed in the MD simulations for 100 and 600 K, but the number of vacancy loops formed due to cascade collapse is small because the PKA energy considered is too low in comparison with ion energy used in experiments. At 100 K none of the vacancy clusters form vacancy loops by cascade collapse, even for a 30-vacancy cluster, but a 24-vacancy cluster was found to collapse to a vacancy loop on a $\{1\,0\,\bar{1}\,0\}$-plane with $\mathbf{b} = 1/2\langle 1\,0\,\bar{1}\,0\rangle$ during the thermal spike at 600 K. Again, this is consistent with the experimental observations. The current modelling of displacement cascades does provide a quantitative description of defect production and clustering in the primary damage state in zirconium, and it would be of interest to extend it to higher energy cascades.

The conclusion from the MD simulations that clustering of both SIAs and vacancies takes place in collision

cascades in zirconium is also consistent with experimental and computer studies of other metals. As discussed recently elsewhere, e.g. [14,18], the fact that the proportion of the total defects retained in clusters and their size distributions are different for the primary interstitial and vacancy clusters, and that these differences are temperature-dependent due to different thermal stabilities, should be taken into account in the modelling of radiation damage effects. The computer simulations performed in this investigation have provided a quantitative description of defect number and configuration in the primary damage state and the dependence of these features on cascade energy and irradiation temperature. These MD results should aid in the understanding of the experimental data for microstructural evolution and property changes that occur during irradiation of α-Zr and its alloys.

## 8. Conclusions

(a) An investigation using MD has been carried out into the effect of lattice temperature on the production of vacancies and interstitial atoms in the primary damage process of displacement cascades with energy up to 20 keV in α-zirconium. The effect of temperature on the thermal spike has been studied quantitatively and is believed to account for several of the effects observed.

(b) The final number of interstitials and vacancies decreases with increasing temperature for a given cascade energy due to the increase in lifetime of the thermal spike at high temperature. The decline in the production efficiency (relative to the NRT estimate) with increasing energy is similar to that found at 100 K, but it is reduced further and saturates at about 20% over the energy range considered.

(c) The power-law dependence of $N_F$ on the energy, $E_p$, of the primary recoil atom $N_F = A(E_p)^m$ is obeyed for cascades in Zr at 100 and 600 K.

(d) The number and size of interstitial and vacancy clusters increase with increasing energy. Clusters containing up to 25 interstitials and 24 vacancies were formed in zirconium by 20 keV cascades at 600 K. The fraction of interstitials in clusters increases with increasing temperature, as a result of the longer thermal spike giving greater assistance to intracascade motion of these defects and the enhanced loss of single interstitials due to recombination.

(e) Most interstitial clusters have the form of a dislocation loop with Burgers vector $1/3\langle 11\bar{2}0\rangle$ , and can glide back and forth by one-dimensional migration along the direction of the Burgers vector. The single interstitials and small clusters of less than four SIAs can occasionally migrate to another basal-plane at 600K. This leads to the enhanced recombination referred to in (b).

(f) The 25-interstitial cluster was also a perfect dislocation loop and extended on the basal and prism-planes that form its glide cylinder.

(g) Collapse of the 24-vacancy cluster to a vacancy dislocation loop on the prism-plane was found to occur during the thermal spike, in contrast to previous results for a 30-vacancy cluster at 100 K. The chance of collapse is increased by the longer lifetime of the thermal spike at higher temperature.

## Acknowledgements

The authors acknowledge the financial support of the CANDU Owners Group (Working Party 32) and the Engineering and Physical Science Research Council in carrying out this research.

## References

[1] D.J. Bacon, T. Diaz de la Rubia, J. Nucl. Mater. 216 (1994) 275.
[2] D.J. Bacon, A.F. Calder, F. Gao, V.G. Kapinos, S.J. Wooding, Nucl. Instrum. and Meth. B 102 (1995) 37.
[3] D.J. Bacon, A.F. Calder, F. Gao, Radiat. Eff. Def. Sol. 141 (1997) 283.
[4] D.J. Bacon, F. Gao, A.V. Barashev, Yu.N. Osetsky, in: V.V. Bulatov, T. Diaz de la Rubia, R. Phillips, E. Kaxiras, N. Ghoniem (Eds.), Symposium, vol. 538, MRS, Pittsburgh, PA, 1998, p. 127.
[5] V. Fidleris, J. Nucl. Mater. 159 (1988) 22.
[6] C. Lemaignan, A.T. Motta, in: B.R.T. Frost (Ed.), Vol. 10 B of Materials Science and Technology; a Comprehensive Treatment, VCH, Weinheim, 1994, p. 1.
[7] S.J. Wooding, D.J. Bacon, W.J. Phythian, Philos. Mag. A 72 (1995) 1261.
[8] S.J. Wooding, D.J. Bacon, Philos. Mag. A 76 (1996) 1033.
[9] S.J. Wooding, L.M. Howe, F. Gao, A.F. Calder, D.J. Bacon, J. Nucl. Mater. 254 (1998) 191.
[10] F. Gao, D.J. Bacon, P.E.J. Flewitt, T.A. Lewis, J. Nucl. Mater. 249 (1997) 77.
[11] G.J. Ackland, S.J. Wooding, D.J. Bacon, Philos. Mag. A 71 (1995) 553.
[12] F. Gao, D.J. Bacon, Philos. Mag. A 80 (2000) 1453.
[13] M.J. Norgett, M.T. Robinson, I.M. Torrens, Nucl. Eng. Design 33 (1975) 50.
[14] B.N. Singh, J.H. Evans, J. Nucl. Mater. 226 (1995) 277.
[15] W.J. Phythian, A.J.E. Foreman, R.E. Stoller, D.J. Bacon, A.F. Calder, J. Nucl. Mater. 223 (1995) 245.
[16] B. Whiting, D.J. Bacon, in: I.M. Robertson, G.S. Was, L.W. Hobbs and T. Diaz de la Rubia (Eds.), Symposium proceedings, vol. 439, Materials Research Society, Pittsburgh, 1997, p. 389.

[17] D.H. Yellen, D.J. Bacon, W.J. Phythian, C.A. English, in: Effects of Irradiation on Materials: 15th International Symposium on ASTM-STP, vol. 1125, 1992, p. 385.
[18] S.I. Golubov, B.N. Singh, H. Trinkhaus, J. Nucl. Mater. 276 (2000) 78.
[19] F. Gao, D.J. Bacon, Yu.N. Oseteky, P.E.J. Flewitt, T.A. Lewis, J. Nucl. Mater. 276 (2000) 213.
[20] Yu.N. Oseteky, D.J. Bacon, A. Serra, B.N. Singh, S.I. Golubov, J. Nucl. Mater. 276 (2000) 65.
[21] A. Jostsons, P.M. Kelly, R.G. Blake, Ninth ASTM International Symposium on Effects of Radiation on Structure Materials, Richland, WA, 1978.
[22] M. Griffiths, J. Nucl. Mater. 159 (1988) 190.
[23] M. Griffiths, Philos. Mag. A 69 (1991) 853.